metals

Article

Low-Temperature Mechanical Behavior of Super Duplex Stainless Steel with Sigma Precipitation

Seul-Kee Kim, Ki-Yeob Kang, Myung-Soo Kim and Jae-Myung Lee *

Department of Naval Architecture and Ocean Engineering, Pusan National University, Busan 609-735, Korea; E-Mails: kfreek@pusan.ac.kr (S.-K.K.); kgyup15@pusan.ac.kr (K.-Y.K.); ms2002korea@pusan.ac.kr (M.-S.K.)

* Author to whom correspondence should be addressed; E-Mail: jaemlee@pusan.ac.kr; Tel.: +82-51-510-2342; Fax: +82-51-512-8836.

Abstract: Experimental studies in various aspects have to be conducted to maintain stable applications of super duplex stainless steels (SDSS) because the occurrence rate of sigma phase, variable temperature and growth direction of sigma phase can influence mechanical performances of SDSS. Tensile tests of precipitated SDSS were performed under various temperatures to analyze mechanical and morphological behavior.

Keywords: super duplex stainless steel; σ phase; sub-zero tensile test; microstructure analysis; microcrack

1. Introduction

Duplex stainless steel (DSS) is a family of stainless steels having intermetallic microstructure consisting of austenite and ferrite phases, which have superior machinability and corrosion resistance, respectively. It is well known that DSS has some superior features such as excellent corrosion resistance and high strength. DSS also has higher pitting resistance equivalent numbers (PREN) than austenitic stainless steels despite of the lower nickel alloy ratio [1–4].

DSS has been widely being used in gas and oil fields. In particular, the high PREN and strength of DSS makes it suitable for harsh industrial fields [5–7]. Super duplex stainless steels (SDSS) are defined as the subset of duplex stainless steels that have a PREN greater than 40. The attractive

combination of mechanical strength and corrosion resistance has led to an increasing number of SDSS applications in harsh environments, mainly in the petrochemical and offshore industries such as pipes, pumps, pressure vessels, separators, and heat exchangers. However, the mechanical and corrosion performance of SDSS can be degraded by undesired phases such as coarse grains and extensive precipitation from the melting and rapid solidification in fusion welding processes. In particular, an inappropriate phase called the sigma phase is fatal to the mechanical performance because it renders SDSS brittle [8–10]. SDSS contains a higher alloying element content than DSS and has a superior corrosion resistance and mechanical performance. However, the sigma phase is more easily generated as the higher level of alloying elements such as Cr and Mo accelerate the kinetics of precipitation [11,12]. Hence, many studies related to effect of sigma phase in DSS and SDSS have been conducted, but most studies of SDSS are focused on only the relationship between the volume fraction of precipitation and the mechanical or corrosive properties [13,14]. However, microcracks have been caused by tensile load in sigma precipitation, it has to be analyzed as the crack has been developed to only vertical direction with tensile loading direction. Hence, in this study, the crack direction and length in the precipitation were compared with the microstructure of SDSS using a scanning electron microscope (SEM).

DSS and SDSS can also be used in low-temperature regions such as chemical and petrochemical environments because it includes half of the austenite phase that acts to halt cleavage propagation dropping the ductile-brittle transient temperature (DBTT). In addition, the austenite phase in DSS or SDSS can transform into the strain-induced martensite phase below temperatures of −50 ℃ [15,16]. In this context, low-temperature tests are needed for SDSS containing a certain amount of precipitation because its mechanical behavior can be changed owing to strain-induced phase transformation. Hence, it is observed how low temperature environment effects to mechanical properties and its microstructure transition of precipitated SDSS in this study.

In petrochemical and marine applications of SDSS, the foregoing situations can occur when prompt cooling cannot be properly performed after the welding process or if the cooling rate is insufficient during manufacture. Therefore, predictions of the occurrence of phase transformation and its behavior are of vital importance. Therefore, the tensile tests in this study were performed under various conditions that could occur in actual use.

Borvik *et al.* (2010) conducted an experimental study of the mechanical behavior of precipitated DSS in low-temperature environments [17]. However, there have been few investigations on the low-temperature behavior of precipitated SDSS. Li *et al.* studied the mechanical properties of SDSS annealed between 500 ℃ and 1100 ℃ K for times ranging between 1 min and 60 min [18]. However, this study does not deal with the temperature effect. In this experimental study, heat treatments for precipitation and tensile tests under sub-zero conditions up to −50 ℃ were performed.

2. Experimental Procedure

2.1. Heat Treatment Process

A UNS S32750 steel was used in this experimental study, and the chemical composition of the super duplex stainless steel (SDSS) is given in Table 1. The as-received hot-rolled steel was

manufactured in a solution annealed state (at 1100 ℃ for 20 min with a heating rate of 1 ℃/s) followed by quenching with water. The homogenized SDSS plate was subsequently cut into six SDSS plates, and each of the cut plates were heated at a rate of 1 ℃/s to an isothermal ageing temperature of 850 ℃. Heat treatment including solution annealing and isothermal ageing was carried out using muffle furnace. To investigate the effect of the ageing period on the microstructure of the SDSS, including the ratio of precipitation of the sigma (σ) phase, the cut plates were homogenized for 5 min, 10 min, 15 min, 30 min, and 60 min after the SDSS reached the setting temperature. One of the cut plates was not exposed to the isothermal ageing process in order to allow for comparison with the other heat-treated plates. After each heating process, the plates were quenched immediately with water. Finally, the six types of precipitated plates were manufactured into tensile specimens in accordance with KS B0801. The dimensions of the tensile specimens are presented in Figure 1. The rod-type tensile test specimens had a gauge length of 50 mm, and 20 tensile specimens under each ageing period were obtained from each cut plate. The heat treatment processes that were applied to the tensile test specimens are summarized in Figure 2.

Table 1. Chemical composition of experimental specimens.

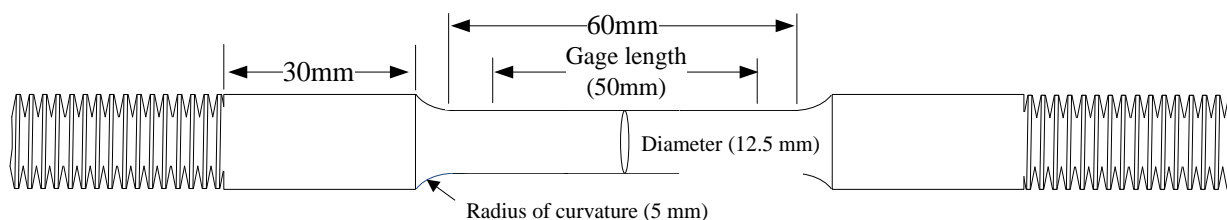| Element (wt. %)	C	Si	Mn	P	S	Ni	Cr	Mo
UNS S32750	0.016 0.017	0.34 0.25	0.44	0.027	0.001	6.8	25.1	4.0

Figure 1. The dimension of the tensile test specimen (KS B0801 10).
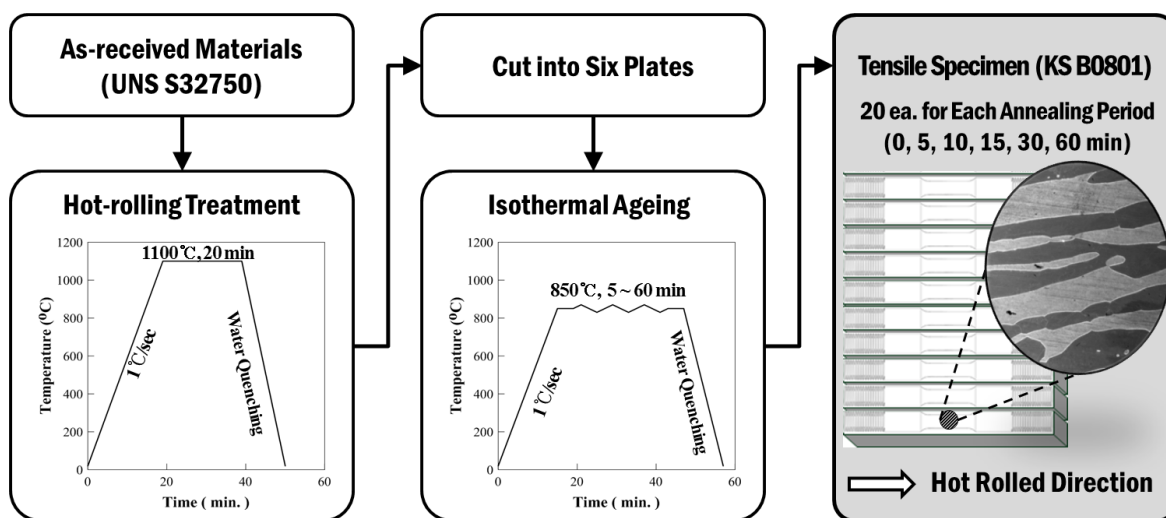

Figure 2. Heat treatment process for precipitation in super duplex stainless steel (SDSS) specimen.

2.2. Tensile Test

A series of tensile tests were performed on the precipitated SDSS specimens at ambient and various low temperatures. Displacement control was applied to the tensile test at all temperatures, and a quasi-static strain rate of 1×10^{-3}/s was applied. Figure 3 shows the experimental apparatus for the series of tensile tests that were conducted in the present study. A universal testing machine (UH-1000kN, Shimadzu, Kyoto, Japan) was equipped with a sub-zero chamber, which enabled the temperature to be maintained in a range of -200 ℃ to 100 ℃ for tensile testing at low temperatures. The schematic of a universal testing machine with a sub-zero chamber is presented in Figure 3a, and a photograph of the testing machine is presented in Figure 3b. Three thermometers were installed in the sub-zero chamber to measure the internal temperature of the chamber. In order to maintain the setting temperature, a digital temperature controller was used to adjust the injection quantity of liquefied nitrogen gas. A cryogenic extensometer, as presented in Figure 3c, was used to measure the strain of the specimen during the tensile test. Specially, the knife edges that were produced were equipped with extensometers, which were embedded on the surface of the rod-type specimen, thus allowing the extensometer to stably hold onto the specimen. The tensile tests for the differently precipitated tensile specimens were carried out under four temperature conditions (20 ℃, 0 ℃, -20 ℃, and -50 ℃) using the aforementioned low-temperature test apparatus.
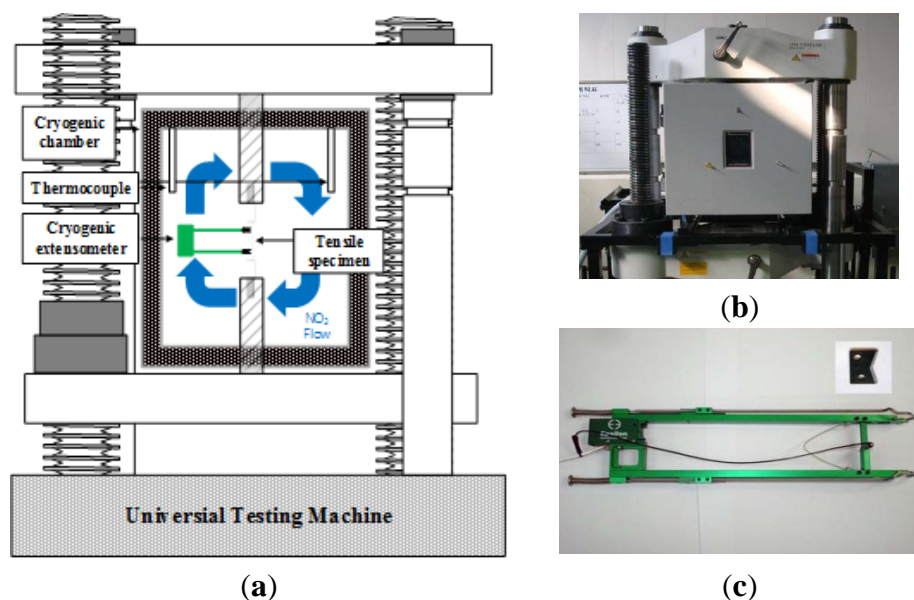

(a) (b) (c)

Figure 3. (**a**) Schematic of custom low temperature test machine; (**b**) photography of universal testing machine; SHIMADZU, UH-1000KNI with cryogenic chamber and (**c**) cryogenic extensometer and knife edge (3542-050M-100-LT).

2.3. Characterization of the Microstructure

In order to investigate the relationship between the characteristics of the microstructure and the mechanical behavior of the precipitated SDSS under a tensile load, half of the fractured specimens were collected as samples. Microstructure analysis was then carried out. The analysis procedure, including the surface treatment of the tested specimens, is presented in Figure 4. The fracture surfaces

were grinded using #100, #200, #300, #600, #1000, #1200, #1500, and #2000 sandpapers. The ground surfaces were then polished to allow for scanning electron microscopy (SEM) characterization. A chemical etching method was performed using aqua regia (1:3 ratio of nitric acid and hydrochloric acid). A field emission-SEM (FE-SEM, SUPRA40 VP, PNUCRF, Busan, Korea) was used to characterize the microstructure. Energy dispersive X-ray spectroscopic (EDX, EDAX, Mahwah, NJ, USA) analysis was also conducted to determine the chemical composition of the various phases [19–21]. The fractional ratio of each phase was calculated based on the ASTM E562 standard [22]. Five FE-SEM images were used to determine the volume fraction of precipitation for each condition.
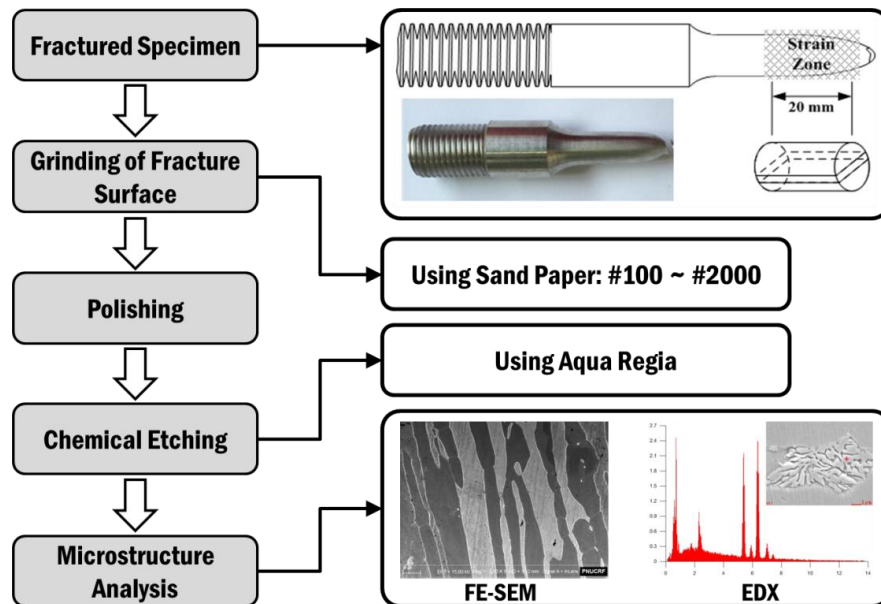

Figure 4. Procedure of microstructure analysis for tested SDSS specimen.

3. Results and Discussion

3.1. Effect of the Isothermal Ageing Treatment

In order to investigate the effect of the isothermal ageing period on the mechanical behavior of the SDSS, the relationships between the nominal stresses and strains under different ageing periods were compared (Figure 5). Most cases that were tested at ambient and low temperature ranges revealed that the material properties, such as yield strength, tensile strength, and elongation, depend significantly on the ageing period. In Figure 5, the specimens that did not undergo ageing treatment (solution annealed state) were found to have a tensile strength of over 800 MPa and elongation of over 0.4. The yield strength and tensile strength of the tensile specimens that were treated by the isothermal process increased with increasing ageing periods. However, in contrast with the relationship between the strength and ageing period, the elongation of the annealed SDSS dramatically decreased with increasing ageing periods. At all of the tested temperatures, these phenomena were distinctly observed. The necking phenomenon was also barely observed in the case where the specimens were treated within 5 min of the ageing period (Figure 6, tested at 20 ℃). This phenomenon was similarly observed at other test temperatures. Therefore, quantitative (elongation) and qualitative (fracture shape) test results revealed that isothermal ageing can lead to embrittlement of SDSS without effect of test temperature.
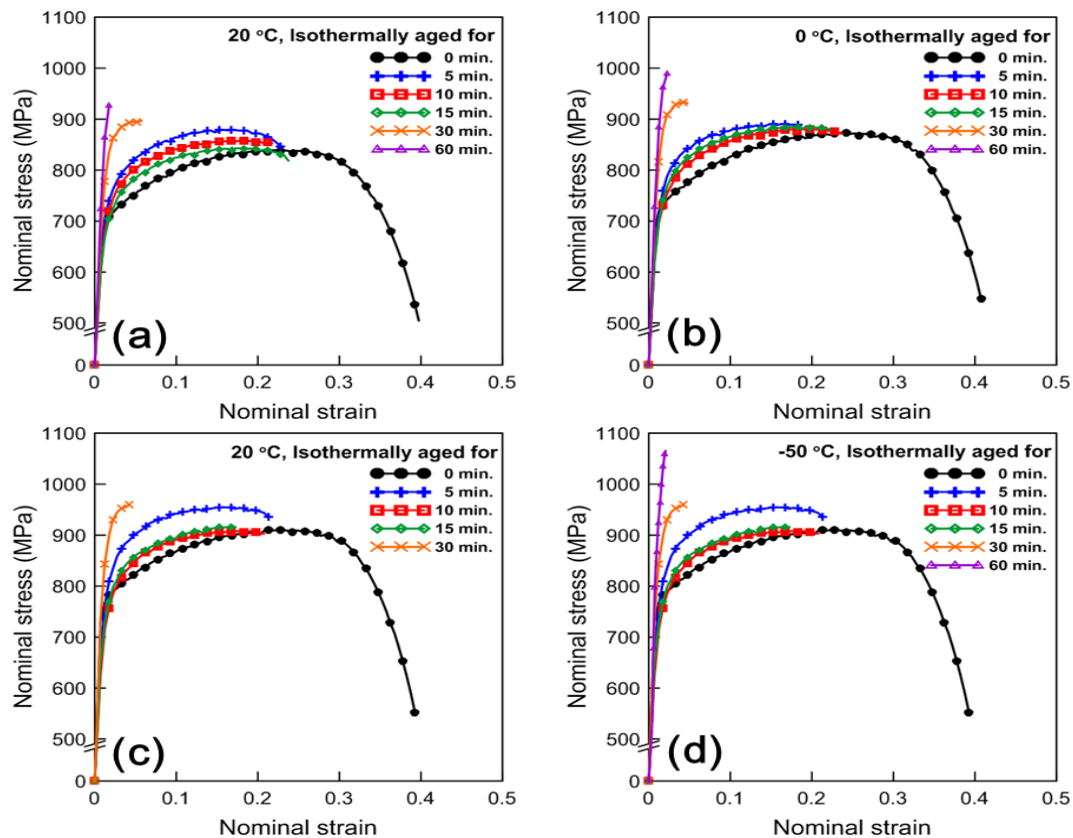
Figure 5. Nominal stress-strain curves of SDSS with tensile test temperature (**a**) 20 ℃; (**b**) 0 ℃; (**c**) −20 ℃ and (**d**) −50 ℃.

(**a**)

(**b**)

(**c**)

(**d**)

Figure 6. *Cont.*

(**e**) 30   (**f**) 60

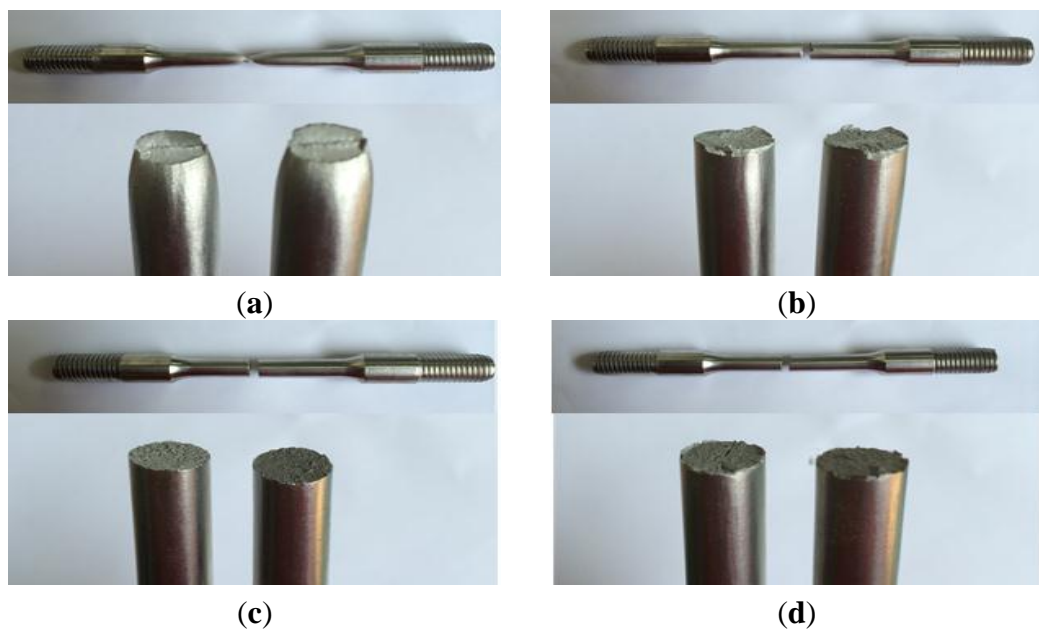**Figure 6.** Comparison of fracture surface of SDSS tensile specimens according to various isothermal ageing periods (tested at 20 ℃). (**a**) 0 min; (**b**) 5 min; (**c**) 10 min; (**d**) 15 min; (**e**) 30 min; (**f**) 60 min.

In order to investigate the changes in the microstructure of the SDSS according to various isothermal ageing periods at 850 ℃, microstructural analyses were carried out. Figure 7 shows representative SEM results of the strain zone of each fractured specimen with four different ageing periods at a test temperature of 20 ℃. Figure 8 and Table 2 also show the EDX analysis results that indicate the chemical composition of each phase on the SDSS as measured using SEM. In the case of a 5-min ageing period, the σ phase did not grow sufficiently as shown in Figure 7a. The flow stress of the tensile test specimen, which was aged for 5 min, increased because the small particles of the σ phase acted as reinforcements in the matrix of the α and γ_2 phases. Therefore, the tensile specimens aged for 5 min increased the strength more than other cases except for over 30 min in spite of loss in ductility when compared with the initial solid heat-treated state as shown in Figure 5.
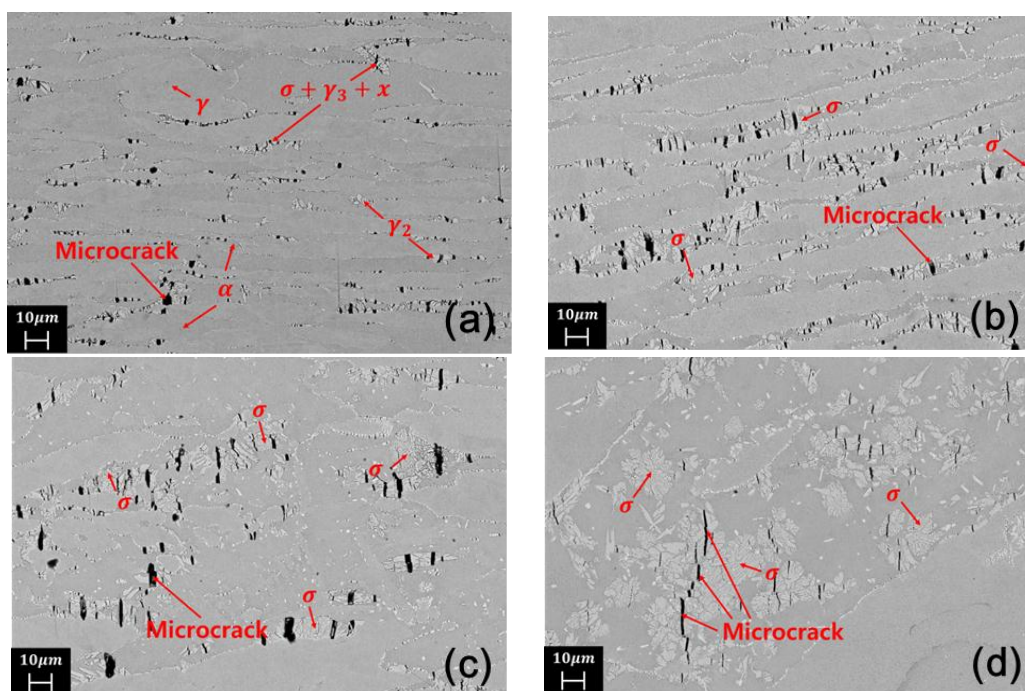

Figure 7. Precipitation of SDSS according various isothermal ageing period (**a**) 5 min; (**b**) 10 min; (**c**) 15 min; and (**d**) 30 min.
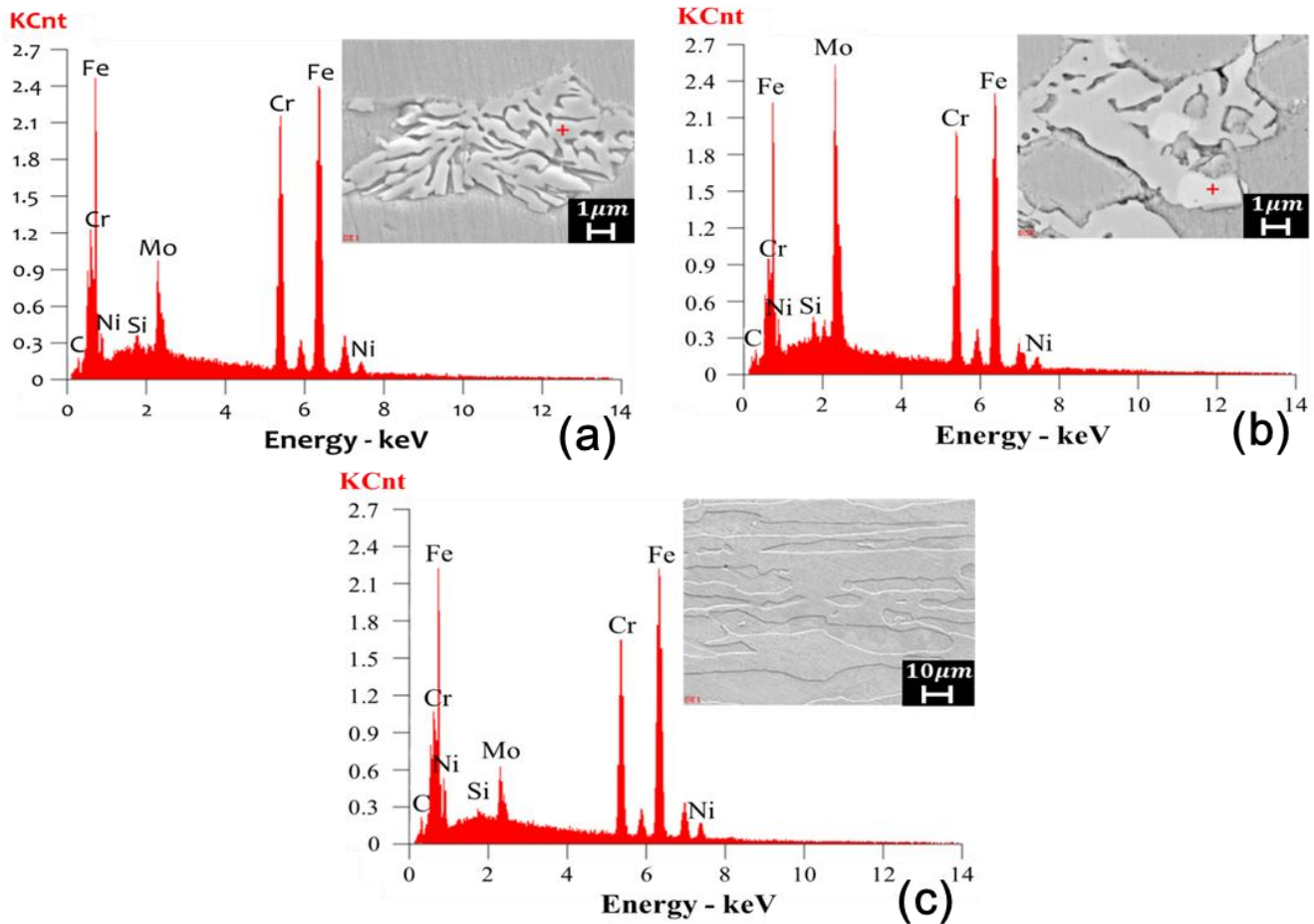
Figure 8. EDX analysis of SDSS (**a**) σ phase; (**b**) χ phase and (**c**) SDSS.

After ageing for more than 5 min at 850 ℃, the σ phases precipitated and grew with prolonged the duration of the ageing period. As shown in Figure 7a, σ, χ, and the newly generated γ phases were precipitated together. The γ_3 particles that were situated in the intervals of the σ phase were generated by nickel enrichment.

Table 2. Chemical composition of σ, χ phase and super duplex stainless steels (SDSS) based on energy dispersive X-ray (EDX) analysis (five minutes of isothermal ageing case).

Element (wt. %)	C	Si	Mo	Cr	Fe	Ni	Volume Fraction (%)
(a) σ phase	1.39	0.53	6.84	28.74	58.41	4.10	3.125
(b) χ phase	1.72	0.69	18.92	25.54	49.65	3.48	11.25
(c) SDSS	2.11	0.42	4.57	25.49	61.33	6.09	-

The grains of the σ and γ_2 phases were stable, and the size of those grains increased with increase in the ageing period. The α and γ_1 phases were bordered by the χ and σ phases and were stretched in the tensile loading direction (Figure 7). The results of the EDX analysis presented in Figure 8 and Table 2 reveal that the σ and χ phases have relatively high molybdenum and chromium content when compared with the other phases. The measured contents of molybdenum on the σ and χ phases as well as the SDSS based on EDX analysis are 6.84, 18.92, and 4.57 wt. %, respectively. The σ and χ phases as well as the SDSS have 28.74, 25.54, and 25.49 wt. % chromium content, respectively. In accordance with

the EDX analysis presented in this study, the precipitated σ and χ phases contained 6~8 and 12~27 wt. % of molybdenum and 29~31 and 17~27 wt. % of chromium, respectively, while previous research found that stainless steel contains 22~28 wt. % of chromium and 3~5 wt. % of molybdenum [23–25]. Because the σ and χ phases contain higher molybdenum and chromium content when compared with the other phases, the toughness and corrosion resistance of the other phases such as the γ and α phases deteriorated owing to the lack of molybdenum and chromium. In particular, a considerable depletion of $γ_3$ was generated when nickel escaped from the χ and σ phases to the outside without chromium and molybdenum [26]. The volume fraction of the σ phase in the case of a 5-min ageing period was measured to be 3% based on ASTM E562 [19].

It is known that the precipitation of the σ and χ phases by isothermal ageing heat treatment occurs in a short time at high temperature ranges. Therefore, the material degradation of the SDSS that leads to fracture also occurs prematurely. As presented in Figure 7, the number of microcracks had dramatically increased with prolonged ageing periods. In the case of 30 min of isothermal ageing, microcracks were considerably propagated through the σ phase. The aforementioned degradation in the material toughness of the SDSS that was induced by the precipitation of the σ phase led to material fracture in spite of the higher ultimate tensile strength caused by precipitation hardening when compared to the solid heat-treated state. This phenomenon is apparently present when isothermal ageing is performed for more than 15 min at 850 ℃. Based on the results of the present study, embrittlement was typically found to begin after (or before) 5 min of ageing at 850 ℃.

3.2. Effect of Testing Temperature

In order to investigate the effect of test temperature on mechanical behavior of the precipitated SDSS, comparison of mechanical properties changed according to test temperature were carried out as presented in the Figure 9. Reduction ration ($R_{elong.}$) presented in Figure 9a can be defined as $R_{elong.}$ = (Elongation at Room Temp. − Elongation)/(Elongation at Room Temp.). $R_{elong.}$ of the specimen aged for 30 min is visibly increased at lower temperatures compared with others (show in Figure 9a). The ultimate tensile stress is synthetically increased by approximately 100–120 MPa by decreasing the temperature from 20 ℃ to −50 ℃. However, the specimens aged for 5 min exhibit different characteristics, as shown in Figure 9b. The tensile strength at 20 ℃ is visibly lower than others. The σ phase affects the tensile strength differently at 20 ℃. The subzero tensile test is more affected by reinforcing effect induced precipitated σ phase.

Strain-induced martensite was not observed in any SEM sample. No phenomena were observed that would change the stiffening tendency while specimens were strained. The occurrence of strain-induced martensite in the austenite phase depends on the chemical composition, strain level, temperature, and strain rate [27,28]. A higher strain rate or lower test temperature are required to observe the strain-induced martensite in SDSS, whether it is isothermally aged or not because the strain rate of the test in the present study was 1×10^{-3}/s and the lowest test temperature was −50 ℃.
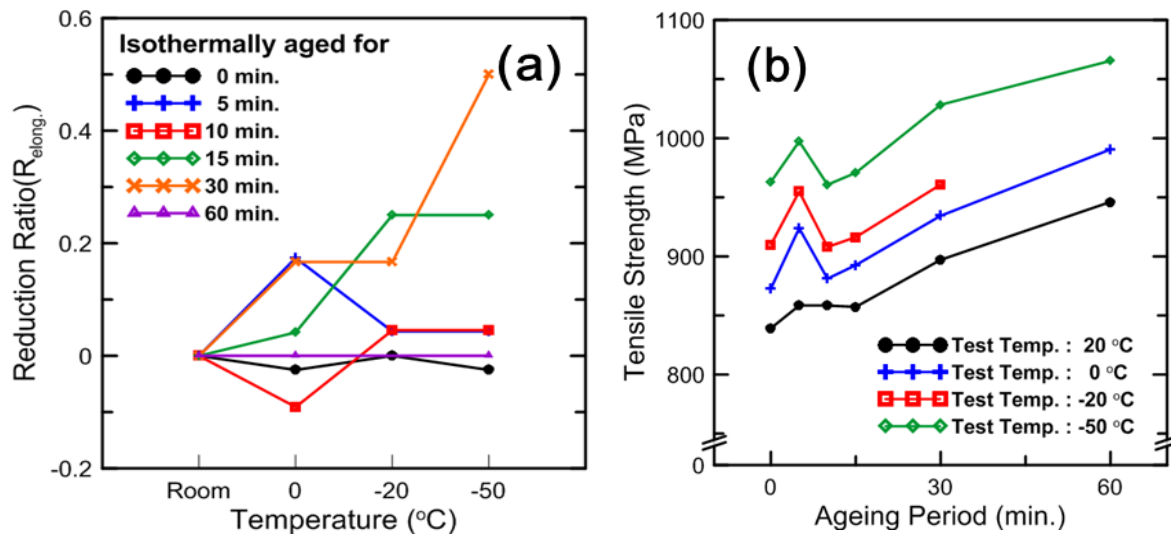
Figure 9. Effect of test temperature on mechanical behavior of the precipitated SDSS: (**a**) elongation and (**b**) tensile strength.

3.3. Effect of Length of the Microcrack

Microcracks propagated through the σ phases in the vertical direction with tensile load in all tests of the precipitated specimen. The crack passed through the entire σ precipitation, which means that the terminated crack length depends on the σ precipitation size (Figure 10). The average microcrack length of each specimen with ageing period is shown in Figure 11. The relationship between volume fraction of the σ phase and length of the microcrack is presented in the Figure 11a. The relationship between the tensile elongation and length of the microcrack is also shown in Figure 11b. Both of those results reveal the similar trend pertaining to length of the microcrack. In accordance with those trends, the tensile elongation of precipitated specimens can be affected by the vertical length of the σ phase. A lower elongation than results of the tested specimen in this study can be measured if tensile test specimens are perpendicularly collected to the tested specimen. This is because the σ phases in the isothermally aged specimens are long in the tensile loading direction. The σ phase grows along the grain boundary in α phase and the initial phase has a long configuration in the loading direction (see Figure 1). The fractographies of the specimens aged for 5 min and 30 min are compared in Figure 6. The fracture surface of the specimen aged for 5 min shows ductility by having a relatively rough surface compared with the specimen aged for 30 min. Therefore, the fracture surface is flatter for longer isothermal ageing period because occurrence of longer microcracks on the larger σ phase reduces the ductile area.
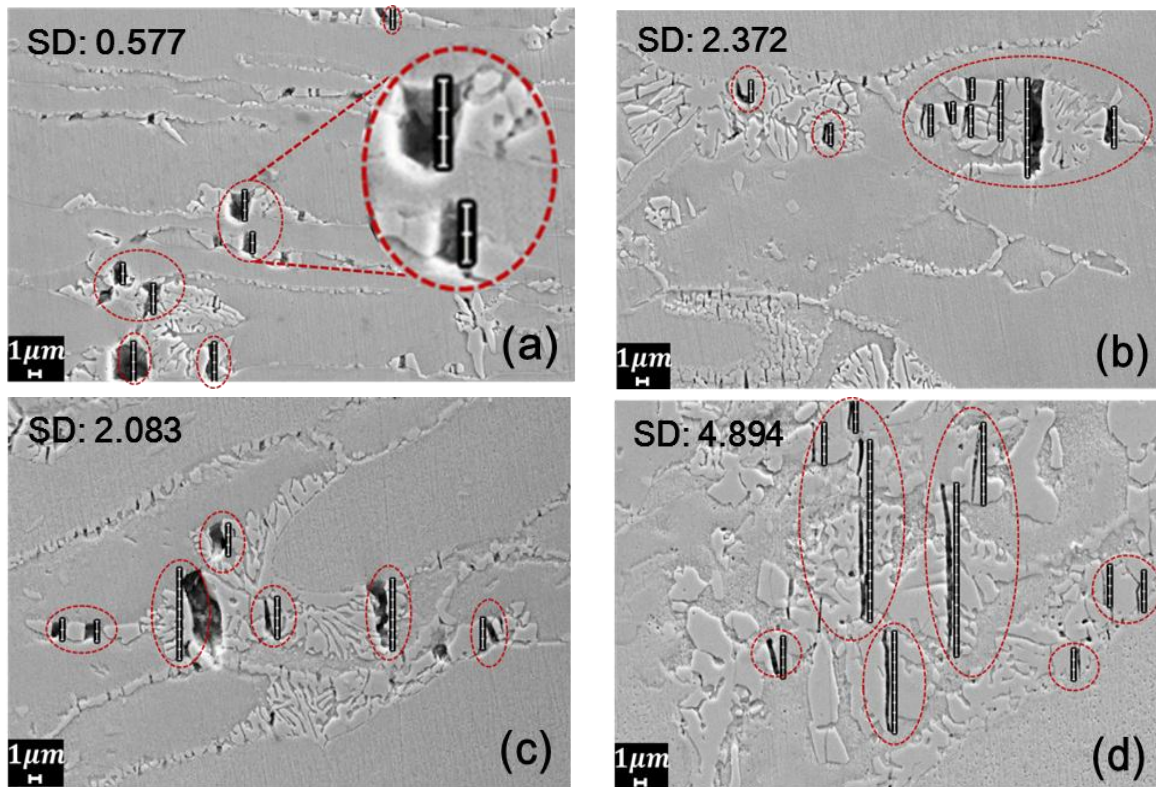
Figure 10. Measuring length of microcracks through the σ the phase caused by tensile test of the specimen annealed for (**a**) 5 min; (**b**) 10 min; (**c**) 15 min; and (**d**) 30 min.
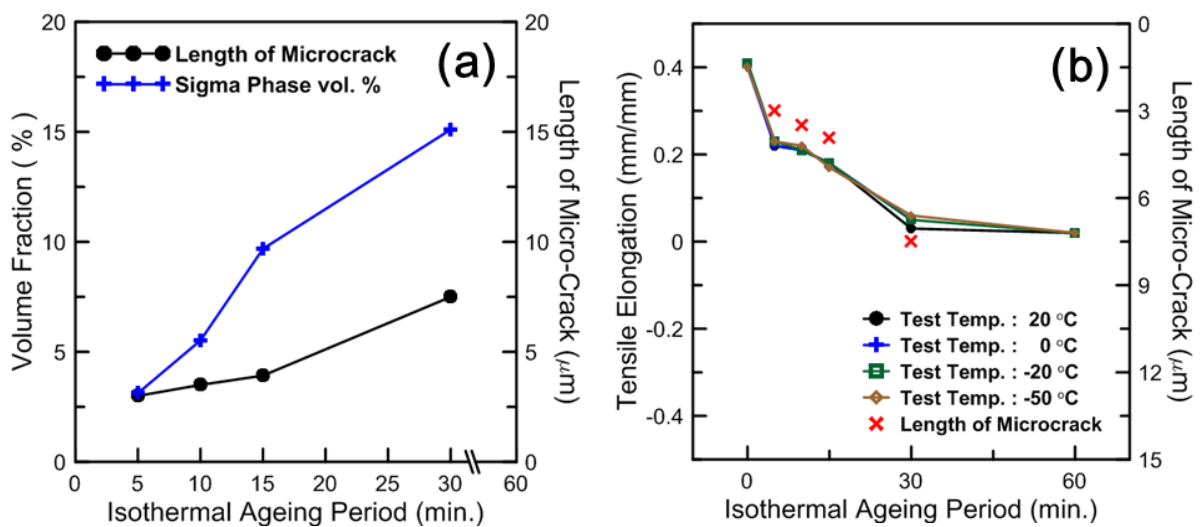

Figure 11. Comparison of the relationship between length of microcrack and (**a**) volume fraction of σ phase and (**b**) tensile elongation according to various test temperatures.

4. Conclusions

The mechanical characteristics of precipitated super duplex stainless steel have been researched through tensile tests by various temperatures and SEM characterizations in this study. A 3 vol. % of σ precipitation reduces the tensile elongation by approximately half but enhances the SDSS by maintaining ductility and increasing tensile strength. It is likely to be more effective at sub-zero

conditions. Microcracks in the σ phase are related to the tensile elongation and fracture surface. The size of the lateral σ surface in the tensile loading direction determines the length of the microcrack and is inversely proportional to the tensile elongation.

No strain-induced martensite was produced in tensile tests at −50 ℃. The decreasing of temperature also equally affects the mechanical behavior of SDSS in the range of 3–20 vol. % as flow stresses increased with lower temperatures in a similar proportion.

Therefore, SDSS containing a σ phase content within 3 vol. % is applicable to the petrochemical industry, provided that sigma phase is grown with loading direction with the occurrence of under 5 μm in a certain application environment. However, these results should be accompanied by fatigue and corrosion tests based on each industrial load and corrosion environment.

Acknowledgments

Author Contributions

Seul-Kee Kim is the first author of the paper and performed the microstructure analysis of the precipitated super duplex stainless steel. Ki-Yeob Kang and Myung-Soo Kim supported experimental tests and microstructure analyses. Jae-Myung Lee is the corresponding author of the paper, and conceived the paper and supervised the experimental tests and microstructure analysis described in the paper.

Conflicts of Interest

The authors declare no conflict of interest.

References

1. Ghosh, S.K.; Mondal, S. High temperature ageing behaviour of a duplex stainless steel. *Mater. Charact.* **2008**, *59*, 1776–1783.
2. Ramkumar, K.D.; Thiruvengatam, G.; Sudharsan, S.P.; Mishra, D.; Arivazhagan, N.; Sridhar, R. Characterization of weld strength and impact toughness in the multi-pass welding of super-duplex stainless steel UNS 32750. *Mater. Des.* **2014**, *60*, 125–135.
3. Linton, V.M.; Laycockb, N.J.; Thomsenb, S.J.; Klumpersb, A. Failure of a super duplex stainless steel reaction vessel. *Eng. Fail. Anal.* **2004**, *11*, 243–256.
4. Liou, H.Y.; Hsieh, R.I.; Tsai, W.T. Microstructure and pitting corrosion in simulated heat-affected zones of duplex stainless steels. *Mater. Chem. Phys.* **2002**, *74*, 33–42.
5. Michalska, J.; Sozańska, M. Qualitative and quantitative analysis of σ and χ phases in 2205 duplex stainless steel. *Mater. Charact.* **2006**, *56*, 335–362.

6. Liou, H.Y.; Hsieh, R.I.; Tsai, W.T. Microstrfucture and stress corrosion cracking in simulated heat-affected zones of duplex stainless steels. *Corros. Sci.* **2002**, *44*, 2841–2856.

7. Iris, A.A. Duplex stainless steels: Brief history and some recent alloys. *Recent Pat. Mech. Eng.* **2008**, *1*, 51–57.

8. Fargas, G.; Mestra, A.; Mateo, A. Effect of sigma phase on the wear behavior of a super duplex stainless steel. *Wear* **2013**, *303*, 584–890.

9. Zhang, W.; Zou, D.; Fan, G.; Li, J. Influence of aging time on sigma phase precipitation in SAF2507 super-duplex stainless steel. *Mater. Sci. Forum* **2009**, *355*, 620–622.

10. Pardal, J.M.; Tavares, S.S.M.; Fonseca, M.C.; de Souza, J.A.; Côrte, R.R.A.; de Abreu, H.F.G. Influence of the grain size on deleterious phase precipitation in superduplex stainless steel UNS S32750. *Mater. Charact.* **2009**, *60*, 165–172.

11. Saeid, T.; Abdollah-zadeh, A.; Assadi, H.; Ghaini, F.M. Effect of friction stir welding speed on the microstructure and mechanical properties of a duplex stainless steel. *Mater. Sci. Eng. A Struct. Mater. Prop. Microstruct. Process.* **2008**, *496*, 262–268.

12. Sieurin, H.; Sandström, R. Sigma phase precipitation in duplex stainless steel 2205. *Mater. Sci. Eng. A* **2007**, *444*, 271–276.

13. De Lacerda, J.C.; Cândido, L.C.; Godefroid, L.B. Effect of volume fraction of phases and precipitates on the mcechanical behavior of UNS S31803 duplex stainless steel. *Int. J. Fatigue* **2015**, *74*, 81–87.

14. Gholami, M.; Hoseinpoor, M.; Moayed, M.H. A statistical study on the effect of annealing temperature on pitting corrosion resistance of 2205 duplex stainless steel. *Corros. Sci.* **2015**, *94*, 156–164.

15. He, J.; Han, G.; Fukuyama, S.; Yokogawa K. Tensile behaviour of duplex stainless steel at low temperatures. *Mater. Sci. Technol.* **1999**, *15*, 909–920.

16. Guocai, C.; Peter, S. Mechanisms for cleavage fracture in duplex stainless steels. In Proceedings of the 13th International Conference on Fracture, Beijing, China, 16–21 June 2013.

17. Borvik, T.; Lange, H.; Marken, L.A.; Langseth, M.; Hopperstad, O.S. Aursand, M.; Rovik, G. Pipe fittings in duplex stainless steel with deviation in quality caused by sigma phase precipitation. *Mater. Sci. Eng. A* **2010**, *527*, 6945–6955.

18. Li, J.; Wu, T.; Riquier, Y. σ phase precipitation and its effect on the mechanical properties of a super duplex stainless steel. *Mater. Sci. Eng. A* **1993**, *174*, 149–156.

19. Sieurin, H.; Sandström, R. Austenite reformation in the heat-affected zone of duplex stainless steel 2205. *Mater. Sci. Eng. A* **2006**, *418*, 250–256.

20. Keshmiri, H.; Momeni, A.; Dehghani, K.; Ebrahimi, G.R.; Heidari, G. Effect of aging time and temperature on mechanical properties and microstructural evolution of 2205 ferritic-austenitic stainless steel. *J. Mater. Sci. Technol.* **2009**, *25*, 597–602.

21. Kashwar, A.; Vennela, N.; Kamath, S.L.; Khatirkar, R.K. Effect of solution annealing temperature on precipitation in 2205 duplex stainless steel. *Mater. Charact.* **2012**, *74*, 55–63.

22. ASTM E562-11. Standard Test Method for Determining Volume Fraction by Systematic Manual Point Count. In *Annual Book of ASTM Standards*; ASTM International: West Conshohocken, PA, USA, 2011.

23. Kiesheyer, H.; Brandis, H. Investigation of phase equilibria in the ternary system Fe–Cr–Mo in solid state. *Int. J. Mater. Res.* **1976**, *67*, 258–263.

24. Jackson, E.; Matthews, L.M. The precipitation kinetics of intermetallic phases in duplex stainless steel and their influence on mechanical properties. In Proceedings of the International Conference on Stainless Steels, Chiba, Japan, 10–13 June 1991.

25. Huhtala, T.; Nilsson, J.O.; Wilson, A. Influence of W and Cu on structural stability in super duplex weld metals. In Proceedings of the 4th International Conferences on Duplex Stainless Steels, Glasgow, UK, 13–16 November 1994; p. 43.

26. Pohl, M.; Storz, O.; Glogowski, T. Effect of intermetallic precipitations on the properties of duplex stainless steel. *Mater. Charact.* **2007**, *58*, 65–71.

27. Park, W.S.; Yoo, S.W.; Kim, M.H.; Lee, J.M. Strain-rate effects on the mechanical behavior of the AISI 300 series of austenitic stainless steel under cryogenic environments. *Mater. Des.* **2010**, *31*, 3630–3640.

28. Okayasu, M.; Fukui, H.; Ohfuji, H.; Shiraishi, T. Strain induced martensite formation characteristics of austenite stainless steel during various loading conditions. *Mater. Sci. Technol.* **2014**, *30*, 301–308.